

Density of states for double-barrier quantum-well structures under the influence of external fields and phase-breaking scattering

A. F. M. Anwar and M. M. Jahan

Electrical and Systems Engineering Department, The University of Connecticut, Storrs, Connecticut 06269-3157

(Received 4 March 1994; revised manuscript received 5 July 1994)

The one-dimensional (1D) density of states (DOS) is calculated self-consistently for double-barrier quantum-well structures in the presence of a perpendicular magnetic field. With the application of a magnetic field, there is a redistribution of the 1D DOS along energy and distance. Contrary to this, an applied electric field results in redistribution mainly along the energy axis. The inclusion of the phase-breaking scattering mechanism diminishes the first peak of the 1D DOS along the energy axis. The total number of states is constant, irrespective of any external (electric or magnetic) fields or phase-breaking scattering.

INTRODUCTION

With the advent of a variety of exotic devices using quantum wells, the various aspects of the tunneling through semiconductors have been studied extensively over the past few years. In this context, the use of magnetic field proves to be a very powerful probe in the understanding of a host of different physical phenomena, e.g., the density of states (DOS), capacitance, conductance etc. The role of the DOS is fundamental¹⁻³ in understanding the transition probabilities, dielectric functions, and absorption and luminescence characteristics in semiconductors. The local DOS provides information about resonant states and gives one a measure of the extent to which the dynamics of transport are dimension dependent.⁴ Moreover, DOS is a much better characteristic of resonant states than transmission coefficient, and it can be applied to more general quantum structures.⁴ Several theoretical and experimental studies have been reported on the DOS of a double barrier quantum well (DBQW). Bahder *et al.*³ showed a smooth transition of DOS from the three-dimensional (3D) square root of energy behavior to the 2D steplike behavior as the height of the barrier is increased. In their formulation, they assumed barriers as delta functions in space. Bruno and Bahder⁴ analyzed 1D DOS with finite barrier width in the absence of any bias voltage. They showed that 1D DOS goes to $E^{-1/2}$ as the height of the barrier goes to zero and to a series of δ functions in the limit of infinite barrier height. Pandey, Sahu, and George⁵ discussed the effect of bias voltage on the global DOS of the quantum well. It was observed that the maxima of the DOS near resonance gets shifted towards low energy as the bias is applied. This is similar to the transmission coefficient behavior, although the two need not be identical.

The fact that the oscillation of the capacitance as a function of magnetic field is directly connected to the DOS at the Fermi energy⁷ has stimulated the experimental determination of the DOS of the quantum structures. Wiess⁷ reported the measurement of the DOS in the presence of a parallel magnetic field. However, to the best of the author's knowledge, the topic of the perpendicular

magnetic-field-induced DOS has not been addressed yet. The present paper presents the calculation of the DOS which may be of great interest in interpreting capacitance and absorbance measurement in quantum structure.

In this paper, the exact space charge distribution of electrons is used self-consistently to calculate quasi-1D DOS in a double-barrier quantum well in the presence of a perpendicular magnetic field. In our model, the barrier is not a delta function in space, rather it can be of any width.¹⁰ The contribution of a perpendicular magnetic field appears in the total Hamiltonian as an effective potential and thus the solution of the Schrödinger equation becomes enormously simplified. The formulation of the 1D DOS follows the scheme proposed by Khondker and Alam.⁶ In the present paper, the main emphasis will be on the effect of the perpendicular magnetic field on the quasi-1D DOS in a DBQW. The effect of phase-breaking scattering is also studied within a first approximation. The total number of states is almost invariant with respect to any perturbation.

THEORY

In the context of DBQW, 1D DOS refers to the number of states available corresponding to a given transverse momentum k_{\perp} . 1D DOS of a DBQW is given as

$$N(x, E_x) = -\frac{2}{\pi} \text{Im}[G^R(x, x, E_x)] , \quad (1)$$

where $G^R(x, x, E_x)$ (Ref. 8) is the retarded Green's function. $G^R(x, x, E_x)$ is the solution of the following Schrödinger equation:⁹

$$\left[E_x - H_0 + \frac{i\hbar}{2\tau_{\phi}(x, E_x)} \right] G^R(x, x_1, E_x) = \delta(x - x_1) . \quad (2)$$

The Hamiltonian $H_0 = (-\hbar^2/2m^*)(d^2/dx^2) + V_b(x)$ is the unperturbed part of the total Hamiltonian and τ_{ϕ} is the phase-breaking time. Here, $V_b(x)$ is the potential due to the conduction-band discontinuity of the DBQW, \hbar is the modified Planck's constant, and m^* is the electronic effective mass. A numerical calculation of the retarded Green's function $G^R(x, x_1, E_x)$ is profoundly intricate.

However, the calculation of DOS necessitates the computation of only the diagonal elements of the retarded Green's function [Eq. (1)] and the off-diagonal elements are unimportant as far as the calculation of 1D DOS is concerned. The diagonal elements of the Green's function can be computed by using the logarithmic derivatives, $Z(x, E_x)$ and is expressed as⁶

$$G^R(x, x, E_x) = \frac{-i4/\hbar}{Z^+(x, E_x) - Z^-(x, E_x)}, \quad (3)$$

where E_x is the longitudinal energy and x is the position. Thus, the 1D DOS is expressed as⁶

$$N(x, E_x) = \text{Im} \left[\frac{i8/\hbar\pi}{Z^+(x, E_x) - Z^-(x, E_x)} \right], \quad (4)$$

where

$$Z(x, x_1, E_x) = \left[\frac{2\hbar}{im^*} \frac{\delta G^R(x, x_1, E_x)/\delta x}{G^R(x, x_1, E_x)} \right]. \quad (5)$$

By using logarithmic derivative $Z = (2\hbar/jm^*)(\psi'/\psi)$, where ψ is the electron wave function and ψ' is the first spatial derivative, the one-electron Schrödinger in the effective-mass approximation can be written as

$$\frac{dZ}{dx} = -j \left[\frac{m^*}{2\hbar} Z^2 + \frac{4}{\hbar} [V_{\text{eff}}(x) - E_x] \right], \quad (6)$$

where $V_{\text{eff}}(x) = V(x) + V_m(x)$ is the effective potential. Here, $V(x)$ accounts for the algebraic summation of the potentials due to applied bias $V_a(x)$, space charge $V_{\text{sc}}(x)$, and $V_b(x)$, $V_m(x) = (m^*/2)\omega_c^2(x - x_0)^2$ is the potential induced due to the application of a magnetic field, $x_0 = \hbar k_y/qB$, $\omega_c = qB/m^*$ is the cyclotron frequency, and q is the elementary particle charge. A value of k_y which maximizes the transmission coefficient of the structure is used in calculating x_0 . The global DOS $N(E_x)$ is obtained by integrating Eq. (4) along the quantum well

$$N(E_x) = \int_0^{L_w} N(x, E_x) dx, \quad (7)$$

where L_w is the length of the quantum well.

The solution of Poisson's equation requires the space charge distribution $n(x)$ inside the quantum well and is given as

$$n(x) = \int_0^\infty dE_x \sum_{\pm} n^{\pm}(x, E_x), \quad (8)$$

where

$$n^{\pm}(x, E_x) = \frac{J^{\pm}(E_x)}{qv_g^{\pm}(x, E_x)} \quad (9)$$

and $J(E_x)$ is the total current density [$J^+(E_x) + J^-(E_x)$], $+$ ($-$) implies that the electron is moving from the emitter (collector) to the collector (emitter) electrode¹¹ and v_g is the electron group velocity and is related to the real part of the logarithmic derivative as¹²

$$v_g^{\pm}(x, E_x) = \frac{1}{2} \text{Re}[Z^{\pm}(x, E_x)]. \quad (10)$$

The updated potential profile is obtained by solving Poisson's equation and is given by

$$\phi(x) = \phi(0) - \frac{q}{\epsilon} \int_0^x dx' \int_0^{x'} n(x'') dx'' \quad (11)$$

and $V_{\text{sc}}(x) = -q\phi(x)$. Equations (6)–(11) are solved until a consistent current is obtained.

RESULTS AND DISCUSSIONS

Results for a symmetric DBQW are presented in this section. The barriers and the quantum well are each 50 Å wide. The barrier height is assumed to be 0.275 eV. The effective mass of the electron is $0.067m_0$ and $0.096m_0$ in the quantum well and in the barrier, respectively, and m_0 is the electron rest mass. The Fermi level E_F is assumed to be 0.03 eV above the bottom of the conduction band of the emitter contact. The calculations are performed for a temperature of 4.2 K.

Figure 1(a) shows the local 1D DOS $N(x, E_x)$ along the quantum well as a function of E_x in the absence of any magnetic field. As observed, $N(x, E_x)$ is a strong function of both x and E_x . $N(x, E_x)$ shows a maxima at the center of the quantum well corresponding to the first eigenenergy, whereas there is a dip at the same location for the second eigenenergy. The observation is reminiscent of the fact that the first and second eigenfunction (or local velocity at those energies) behave accordingly. At intermediate energies, $N(x, E_x)$ depends upon the joint contribution of the first and second eigenstates. With the application of magnetic field, some new features are observed in the 1D DOS plot as shown in Fig. 1(b). $N(x, E_x)$ at the first resonant energy shows, unlike the previous case, a variation with x . The departure of the behavior of $N(x, E_x)$ along the x axis can be explained both classically and quantum mechanically. Classically, the number of periods along the x axis is given by the ratio L_w/L_B , where $L_B = 2\hbar k_F/qB$, k_F is the Fermi wave number, and L_w is the length of the quantum well. With increasing magnetic field, L_B decreases and hence L_w/L_B increases to introduce more oscillation. This is indeed the case as shown in the figure. At 20 T, $L_w/L_B = 2$ and this equals the number of periods of $N(x, E_x)$ along the distance at the first eigenenergy. A similar conclusion can be drawn by applying the time-independent perturbation theory to the present problem. Provided the perturbation H' is relatively small (which is the case for small magnetic field) the perturbed first eigenfunction can be written as

$$\psi_1^{\pm} = \psi_0^{\pm} \sum_{i=2}^{\infty} c_i \psi_0^i,$$

where ψ_0^i is the unperturbed i th eigenfunction and the coefficient c_i is $c_i = \langle \psi_0^i | H' | \psi_0^{\pm} \rangle / (E_1 - E_2)$. Therefore, in the presence of an applied magnetic field, the eigenstates are a linear combination of all other states and is evident in $N(x, E_x)$ plot. The full width at half maximum (FWHM) of $N(x, E_x)$ versus E_x plot carries the signature of the FWHM of the transmission coefficient plot as a function of E_x . The FWHM of $N(x, E_x)$, therefore, is related to the lifetime τ of the carriers (FWHM $\sim 1/\tau$).

The behavior of DOS in the crossed electric and magnetic field is studied next. The application of a bias voltage introduces a term $-q\mathcal{E}x$ into the unperturbed Hamiltonian H_0 . Here, \mathcal{E} is the electric field corresponding to the bias voltage and x is the distance. Contrary to this, the application of a perpendicular magnetic field modifies the unperturbed Hamiltonian with a term $V_m(x) = q(m^*/2)\omega_c^2(x-x_0)^2$. Thus, the presence of these two mutually counteracting factors in the total Hamiltonian try, if not completely, to cancel each other. Figure 1(b) [Fig. 1(c)] shows $N(x, E_x)$ along the quantum well as a function of E_x for $B=20$ T and $V_a=0$ V (0.05 V). It is observed that Fig. 1(c) resembles Fig. 1(a) ($B=0$ T) more closely than does Fig. 1(b). Thus, the application of crossed electric and magnetic field mutually counteracts each other.

The influence of the phase-breaking scattering (i.e., τ_ϕ is finite) is also studied in the context of the behavior of the 1D DOS. Figure 1(d) shows $N(x, E_x)$ as a function of both distance x and energy E_x for $B=0$ T and $V_a=0$ V for finite τ_ϕ . As is apparent, the peak in Fig. 1(a) corresponding to the first eigenenergy becomes drastically smeared out in Fig. 1(d). In order to appreciate this feature more clearly, the behavior of $N(x, E_x)$ as a function of E_x at the center of the well with τ_ϕ as a parameter is plotted in Fig. 2. Thus although the peak of DOS at the first eigenenergy gets smeared out in the presence of

the phase-breaking scattering, the peak at the second eigenenergy remains essentially unaffected. The presence of the phase-breaking scattering results in a redistribution of DOS by depleting the states from the first eigenstates to the intermediate energies between the first and second eigenstates. It is to be noted that τ_ϕ is, in general, inversely proportional to $N(x, E_x)$. Thus, a self-consistent solution for $N(x, E_x)$ demands a self-consistent calculation for τ_ϕ and is obtained in the following manner. Initially τ_ϕ is assumed to be 1 ps.¹⁰ $N(x, E_x)$ are calculated by using Eqs. (2)–(4) and τ_ϕ 's were updated by using the calculated $N(x, E_x)$. The updated τ_ϕ 's were used in the next iteration to recalculate $N(x, E_x)$. The process was repeated until the change in $N(x, E_x)$ between two successive iterations becomes very small. The constant of proportionality C [$\tau_\phi = C/N(x, E_x)$] was calculated by assuming $\tau_\phi = 1$ ps at the first eigenenergy. The value of τ_ϕ specified in the plot is that corresponding to the peak DOS. As expected,⁶ the first peak is gradually washed out with decreasing τ_ϕ . The application of a magnetic field in this case introduces an additional redistribution of DOS of the structure by slightly weakening the effect of the phase-breaking scattering.

In Fig. 3, the global 1D DOS is plotted as a function of E_x with magnetic field as a parameter. Depending on the magnetic field, the peaks of $N(x, E_x)$ at resonance vary.

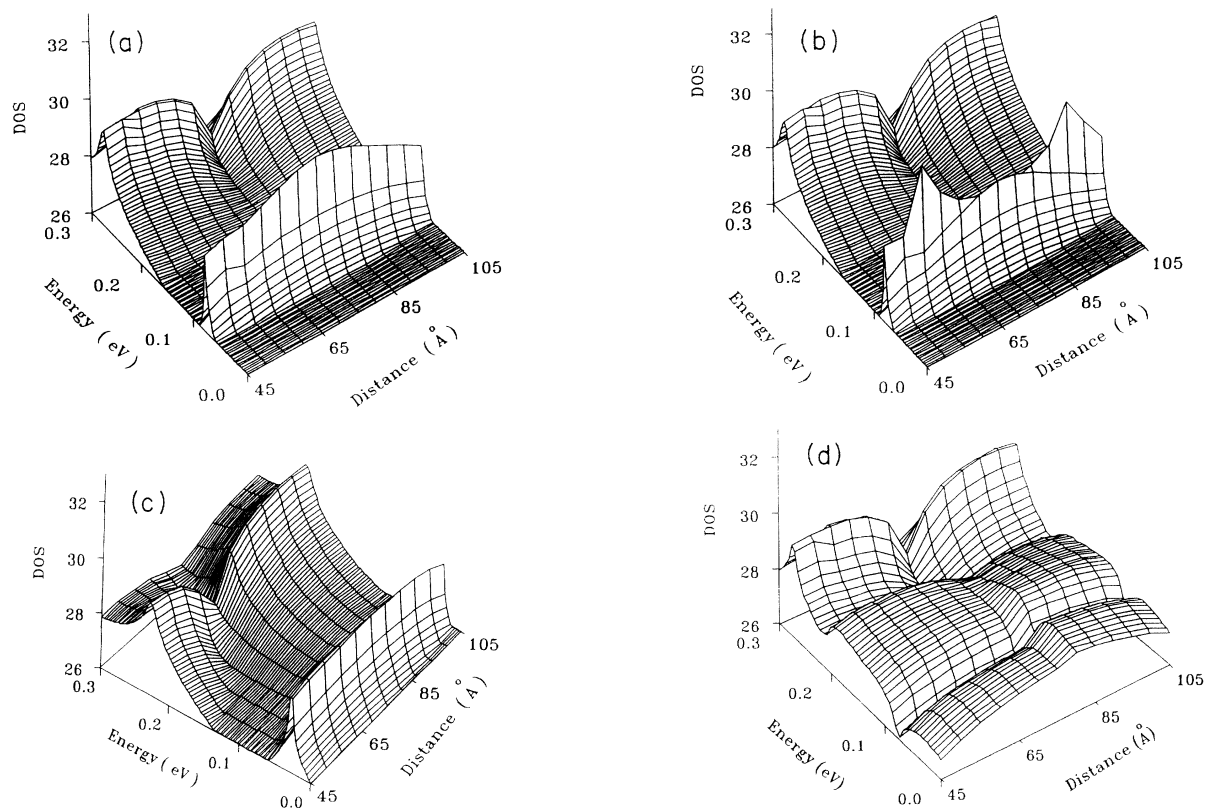


FIG. 1. The base-10 log of the local DOS $N(x, E_x)$ (per cubic meter per joule) is plotted along the quantum well as a function of E_x . (a) corresponds to $B=0$ T. (b) and (c) correspond to $B=20$ T. V_a is assumed 0 for (a) and (b), and 0.05 V for (c). $\tau_\phi = \infty$ is assumed. (d) shows the behavior of $N(x, E_x)$ for self-consistently calculated τ_ϕ .

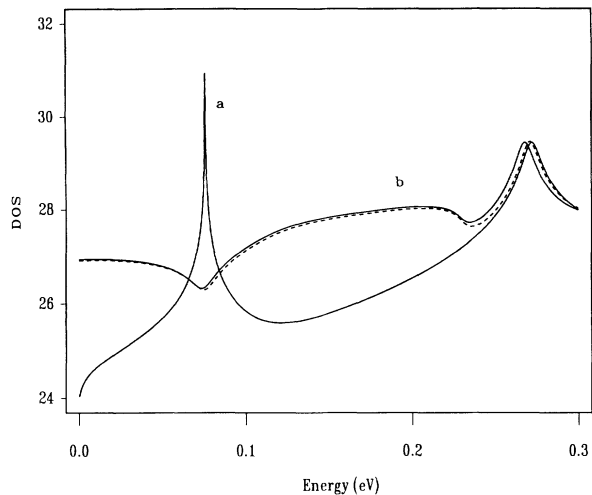


FIG. 2. The base-10 log of local DOS $N(x, E_x)$ (at the center of the quantum well) is plotted as a function of E_x with τ_ϕ as a parameter. Curves *a* and *b* correspond to $\tau_\phi = \infty$ and 10^{-12} sec, respectively, and $B = 0$ T. Broken curve shows the result for $B = 20$ T and $\tau_\phi = 10^{-12}$ sec.

In order to comprehend the implication of the figure, the area under the curve is calculated using an effective 1D DOS, $N_{\text{eff}}(E_x) = N(E_x) / (1 + e^{(E_F - E_x)/kT})$. An integration of $N_{\text{eff}}(E_x)$ over E_x from 0 to ∞ will yield the total number of states. The inclusion of the phase-breaking scattering mechanism diminishes the number of states at the first eigenenergies. Irrespective of the applied magnetic field or electric field or the presence of phase-breaking scattering, the integration gives a value of 5×10^{12} . This proves the fact that states can be neither created nor annihilated by applying external perturbation. This effect may be observed experimentally by probing the capacitance of the structure which carries the signature of the DOS of the DBQW.⁷

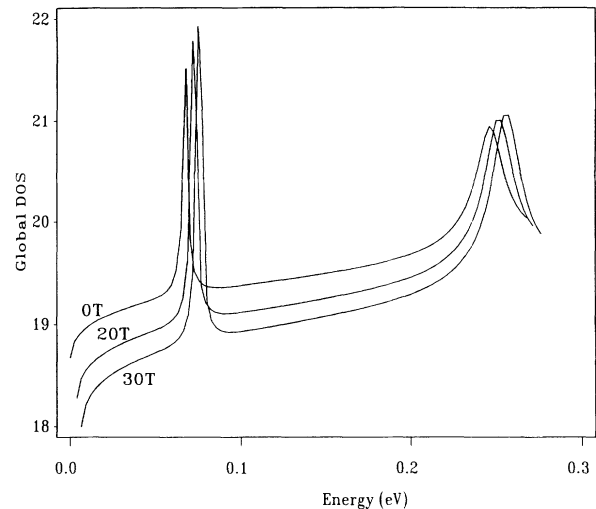


FIG. 3. The base-10 log of global DOS (per square meter per joule) is plotted as a function of E_x with magnetic field as a parameter.

CONCLUSION

The 1D DOS is calculated for a DBQW by calculating the diagonal elements of retarded Green's function. The application of magnetic field modifies the 1D DOS as a function of both energy and distance in the quantum well. The application of crossed electric and magnetic field counteracts the effects of each other, if not completely. In the presence of magnetic field, the peak of the global DOS shifts to higher energy and the FWHM in the neighborhood of the eigenenergies gets modified. The total number of states, independent of the origin of perturbation (electric, magnetic, or phase-breaking scattering), remains constant.

¹G. Kim and G. B. Arnold, Phys. Rev. B **38**, 3252 (1988).

²A. Isihara and K. Ebina, Solid State Phys. **21**, 1079 (1988).

³T. B. Bahder, J. D. Bruno, R. G. Hay, and C. A. Morrison, Phys. Rev. B **37**, 6256 (1988).

⁴J. D. Bruno and T. B. Bahder, Phys. Rev. B **39**, 3659 (1989).

⁵L. N. Pandey, D. Sahu, and T. F. George, Appl. Phys. Lett. **56**, 277 (1990).

⁶A. N. Khondker and M. A. Alam, Phys. Rev. B **45**, 8516 (1992).

⁷V. Gudmundsson and R. R. Gerhardt, Phys. Rev. B **35**, 8005 (1987); D. Weiss, in *Science and Engineering of One- and Zero-Dimensional Semiconductors*, Vol. 214 of NATO Ad-

vanced Study Institute, Series B: Physics, edited by Steven P. Beaumont and Clivia M. Sotomayor Torres (Plenum, New York, 1983), p. 221.

⁸L. V. Keldysh, Zh. Eksp. Teor. Fiz **47**, 1515 (1964) [Sov. Phys. JETP **20**, 1018 (1965)].

⁹M. J. McLennan, Y. Lee, and S. Datta, Phys. Rev. B **43**, 13 846 (1991).

¹⁰Y. Lee, M. J. McLennan, and Supriyo Datta, Phys. Rev. B **43**, 14 333 (1991).

¹¹M. Alam and A. N. Khondker, J. Appl. Phys. **68**, 1196 (1990).

¹²A. F. M. Anwar, A. N. Khondker, and M. R. Khan, J. Appl. Phys. **65**, 2761 (1989).